

simplify the form of the coupled equations, also provides a spurious centrifugal potential. It seems that this extra potential serves inadvertently to simulate the effect of the nonadiabatic terms we have discussed above, and hence to eliminate the resonance.

An interesting question may be raised now concerning the Ps-He<sup>+</sup> channel in e<sup>+</sup>-He scattering. This system is the same as Ps-p at large distances, but its additional Van der Waals attraction might be just enough to produce the resonance. The cross section near threshold for e<sup>+</sup>-He scattering has been measured,<sup>15</sup> although the

<sup>15</sup> S. Marder, V. W. Hughes, C. S. Wu, and W. Bennett, *Phys. Rev.* **103**, 1258 (1956); W. B. Teutsch and V. W. Hughes, *ibid.* **103**, 1266 (1956).

analysis of the experiment is not straightforward. It is possible that a resonance near threshold is needed to bring about agreement between experiment<sup>15</sup> and theory.<sup>16</sup>

#### ACKNOWLEDGMENTS

All the numerical results reported here were programmed by Edward Monasterski and were computed using the IBM 360 at the Laboratory for Theoretical Studies.

<sup>16</sup> R. J. Drachman, *Phys. Rev.* **144**, 25 (1966); N. R. Kestner, J. Jortner, M. H. Cohen, and S. A. Rice, *ibid.* **140**, A56 (1965).

## Measurement of High-Energy Charge-Transfer Cross Sections for Incident Protons and Atomic Hydrogen in Various Gases\*

L. H. TOBUREN,<sup>†</sup> M. Y. NAKAI,<sup>‡</sup> AND R. A. LANGLEY  
Oak Ridge National Laboratory, Oak Ridge, Tennessee 37830  
(Received 8 February 1968)

Measurements of electron-capture cross sections  $\sigma_{10}$  and electron-loss cross sections  $\sigma_{01}$  for protons and atomic hydrogen in H<sub>2</sub>, He, Ar, Kr, N<sub>2</sub>, O<sub>2</sub>, CO, CO<sub>2</sub>, H<sub>2</sub>O, CH<sub>4</sub>, C<sub>2</sub>H<sub>4</sub>, C<sub>2</sub>H<sub>6</sub>, and C<sub>4</sub>H<sub>10</sub> are reported and compared with published theoretical estimates and experimental results. The energy range was 100 to 2500 keV. The results are presented in graphical form. By applying the additive rule, the cross sections  $\sigma_{10}$  and  $\sigma_{01}$  are estimated for hydrogen particles in carbon.

### I. INTRODUCTION

A SUMMARY of experimental results of charge-transfer processes prior to 1958, for incident-particle energies less than 1.0 MeV, has been published by Allison.<sup>1</sup> A paper by Welsh *et al.*<sup>2</sup> reviews some of the charge-transfer results subsequent to 1958. Measurements by Welsh *et al.*,<sup>2</sup> Williams,<sup>3</sup> and Schryber<sup>4</sup> have extended the energy range for the various cross sections up to 13.8 MeV for the target gases H<sub>2</sub>, He, Ar, and N<sub>2</sub>.

Reviews of various theoretical formulations used in calculating charge-transfer cross sections have been presented by Bates and McCarroll,<sup>5</sup> Bates,<sup>6</sup> Dalgarno,<sup>7</sup>

and Bates and Williams.<sup>8</sup> Of particular interest to the present experiment are recent papers in which electron-capture cross sections have been calculated for protons on N, O, Ar, and Kr targets. Mapleton<sup>9,10</sup> has calculated cross sections for the capture of 2*p* electrons from atomic nitrogen and oxygen by means of the first Born approximation. He has also extended the first Born calculation to include capture from inner electron shells.<sup>11</sup> A first Born approximation has been applied by Nikolaev<sup>12</sup> to calculate the cross section for electron capture by protons in hydrogen, helium, lithium, nitrogen, neon, argon, and krypton. This calculation includes contributions to the cross section from inner electron shells of the target atom. Bates and Mapleton<sup>13</sup> have used a classical approach to calculate the electron-capture cross sections as a function of the atomic parameters of the target. This classical approach does not include the possibility of electron capture from inner

\* Research sponsored by the U. S. Atomic Energy Commission under contract with the Union Carbide Corporation.

<sup>†</sup> Present address: Battelle Northwest, Richland, Wash. The results presented here were included in a thesis submitted by L. H. Toburen to the faculty of Vanderbilt University in partial fulfillment of the requirements for the degree of Doctor of Philosophy.

<sup>‡</sup> Present address: Osaka Laboratory, Atomic Energy Research Institute, 508 Mii, Neyagawa-City, Osaka, Japan.

<sup>1</sup> S. K. Allison, *Rev. Mod. Phys.* **30**, 1137 (1958).

<sup>2</sup> L. M. Welsh, K. H. Berkner, S. N. Kaplan, and R. V. Pyle, *Phys. Rev.* **158**, 85 (1967).

<sup>3</sup> J. F. Williams, *Phys. Rev.* **157**, 97 (1967).

<sup>4</sup> U. Schryber, *Helv. Phys. Acta* **39**, 562 (1966).

<sup>5</sup> D. R. Bates and R. McCarroll, *Advan. Phys.* **11**, 39 (1962).

<sup>6</sup> D. R. Bates, in *Atomic and Molecular Processes*, edited by D. R. Bates (Academic Press Inc., New York, 1962), p. 549.

<sup>7</sup> A. Dalgarno, in *Atomic and Molecular Processes*, edited by M. R.

C. McDowell (North-Holland Publishing Co., Amsterdam, 1964), p. 609.

<sup>8</sup> D. R. Bates and A. Williams, *Proc. Phys. Soc. (London)* **A70**, 306 (1957).

<sup>9</sup> R. A. Mapleton, *Phys. Rev.* **130**, 1829 (1963).

<sup>10</sup> R. A. Mapleton, *Proc. Phys. Soc. (London)* **85**, 1109 (1965).

<sup>11</sup> R. A. Mapleton, *Phys. Rev.* **145**, 25 (1966).

<sup>12</sup> V. S. Nikolaev, *Zh. Eksperim. i Teor. Fiz.* **51**, 1263 (1966)

[English transl.: *Soviet Phys.—JETP* **24**, 847 (1967)].

<sup>13</sup> D. R. Bates and R. A. Mapleton, *Proc. Phys. Soc. (London)* **87**, 657 (1966).

shells and therefore is not expected to give satisfactory results at energies above 500 keV where inner-shell capture becomes significant. An extension of this calculation has been made<sup>14</sup> to include capture from the inner electron shells of argon.

## II. EXPERIMENTAL METHOD AND MATHEMATICAL FORMULATION

The charge-transfer cross sections were measured by passing a single-charge-state hydrogen beam through a gas cell. The beam interacted with the gas in the cell and emerged as a multiple-charge-state beam. This beam was charge analyzed by applying a voltage to a set of condenser plates and measuring the intensity of each charge state. The rate of increase of a charge state as the gas cell pressure increased gave a measure of the appropriate cross section.

A general mathematical description which includes a description of this method of measurement has been formulated by Allison.<sup>1</sup> At incident-particle energies above 75 keV the cross section for the formation of  $H^-$  is negligible in comparison with  $\sigma_{10}$  and  $\sigma_{01}$ , so that a two-component charge system may be assumed. With this approximation, closed solutions are given as

$$F_f = \frac{\sigma_{if}}{\sigma_{if} + \sigma_{fi}} \{1 - \exp[-\alpha P(\sigma_{if} + \sigma_{fi})]\}. \quad (1)$$

$F_f$  is the ratio of the intensity of the charge-changed component of charge  $f$  to the intensity of the initial beam with single charge  $i$ ;  $\sigma_{if}$  is the cross section for a charge-changing collision, where  $i$  is the charge state of the beam particle before interaction and  $f$  is the charge state after interaction;  $P$  is the pressure of the gas cell;  $\alpha$  is given by

$$\alpha = N_L l / RT, \quad (2)$$

where  $N_L$  is Loschmidt's number,  $R$  is the gas constant,  $T$  is the absolute temperature, and  $l$  is the effective path length of the beam in the gas cell.

The data from which the cross sections were calculated were obtained under "thin" target (single collision) conditions; such that the exponent in Eq. (1) was small and the exponential could be expanded in a power series. If higher orders are neglected, Eq. (1) can be written as

$$F_f = \alpha \sigma_{if} P. \quad (3)$$

The fraction  $F_f$  was determined experimentally from the measured intensities of the components of the transmitted beam

$$F_f = \frac{I_{Hf}}{I_{H_i} + I_{Hf}}. \quad (4)$$

The fraction  $F_f$  was measured for several values of the

target gas pressure  $P$ , and the results were plotted as  $F_f$  versus  $P$ . This plot resulted in a straight line under "thin" target conditions and the slope of the straight line was proportional to the cross section  $\sigma_{if}$  as indicated by Eq. (3).

The equilibrium fraction is defined as

$$F_{f\infty} = \lim_{P \rightarrow \infty} F_f = \frac{\sigma_{if}}{\sigma_{if} + \sigma_{fi}}. \quad (5)$$

$F_{f\infty}$  represents the fraction of ions of charge  $f$  in the beam after it has undergone a sufficient number of collisions so that no further change in charge composition can be detected. The equilibrium fractions  $F_{1\infty}$  and  $F_{0\infty}$  were measured and compared with the measured cross

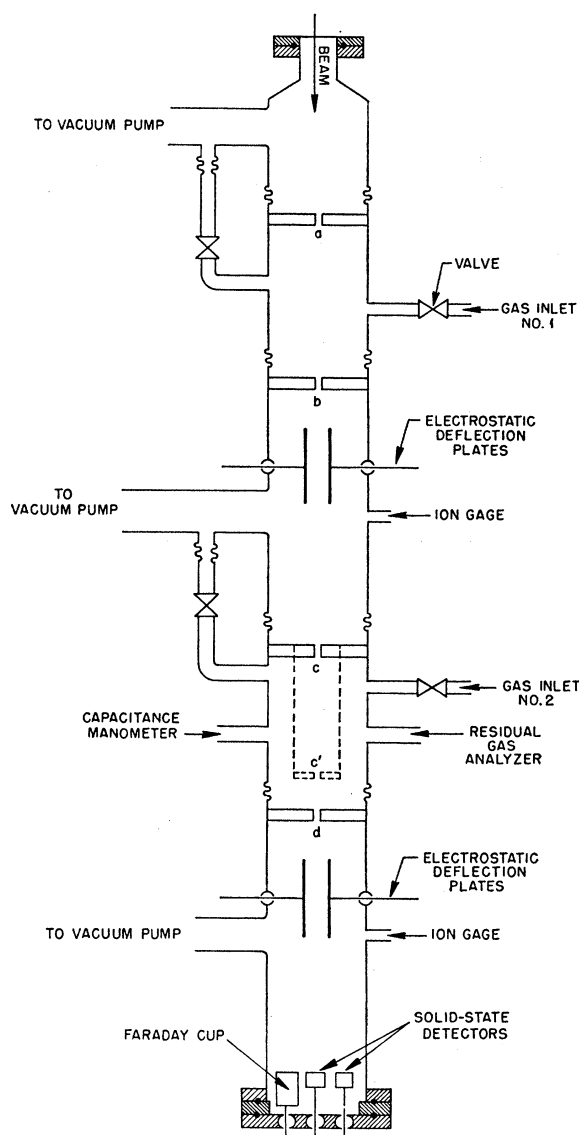


FIG. 1. Schematic drawing of the apparatus.

<sup>14</sup> D. R. Bates and R. A. Mapleton, Proc. Phys. Soc. (London) 90, 909 (1967).

sections  $\sigma_{10}$  and  $\sigma_{01}$  as a check of the internal consistency of the experiment.

Collision cells with path lengths of  $3.06 \pm 0.06$  and  $17.50 \pm 0.06$  in. were used in this work which resulted in different values of  $\alpha$  in Eq. (2). The cross sections quoted in Sec. V are an average of values obtained from each collision cell.

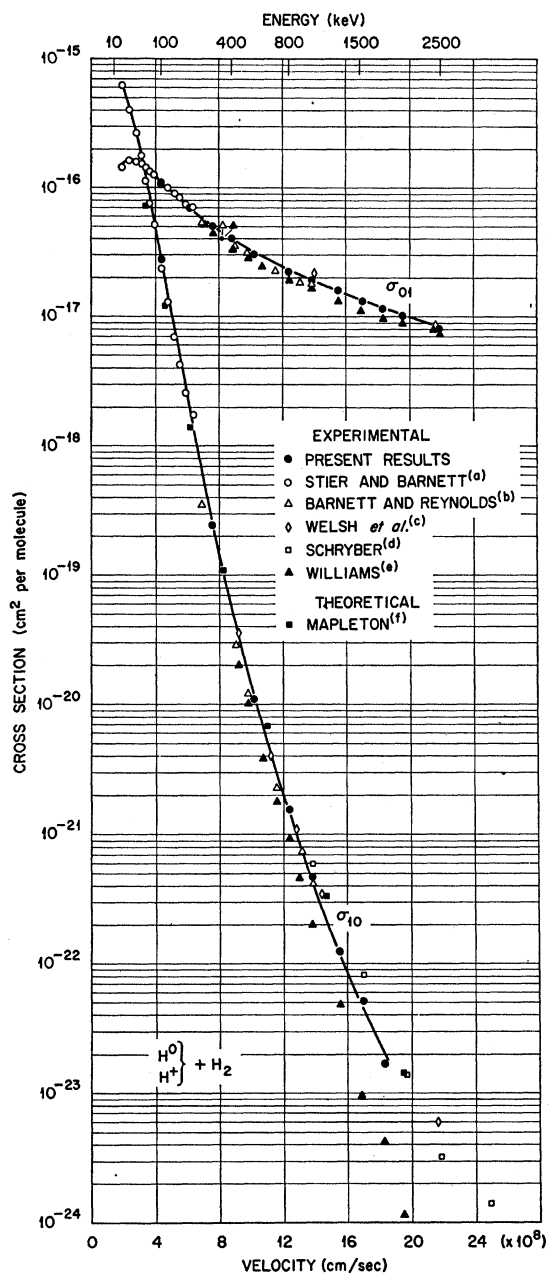


FIG. 2. Single-electron capture and loss cross sections for protons and atomic hydrogen, respectively, on hydrogen with previous experimental and theoretical values. Experimental results: (a) see Ref. 17, (b) see Ref. 18, (c) see Ref. 2, (d) see Ref. 4, and (e) see Ref. 3. Theoretical results: (f) see Ref. 20. The electron-capture cross sections reported by Williams have been multiplied by a factor of 2 (see Ref. 18).

### III. APPARATUS

Two proton accelerators were used to cover the energy range of the present measurement. For the low-energy measurements (100 to 600 keV), protons were accelerated by a conventional high-voltage supply. The voltage had been calibrated to  $\pm 2$  keV at 340 and 483 keV by using the  $^{19}\text{F}(p,\alpha\gamma)$  resonances. The high-energy

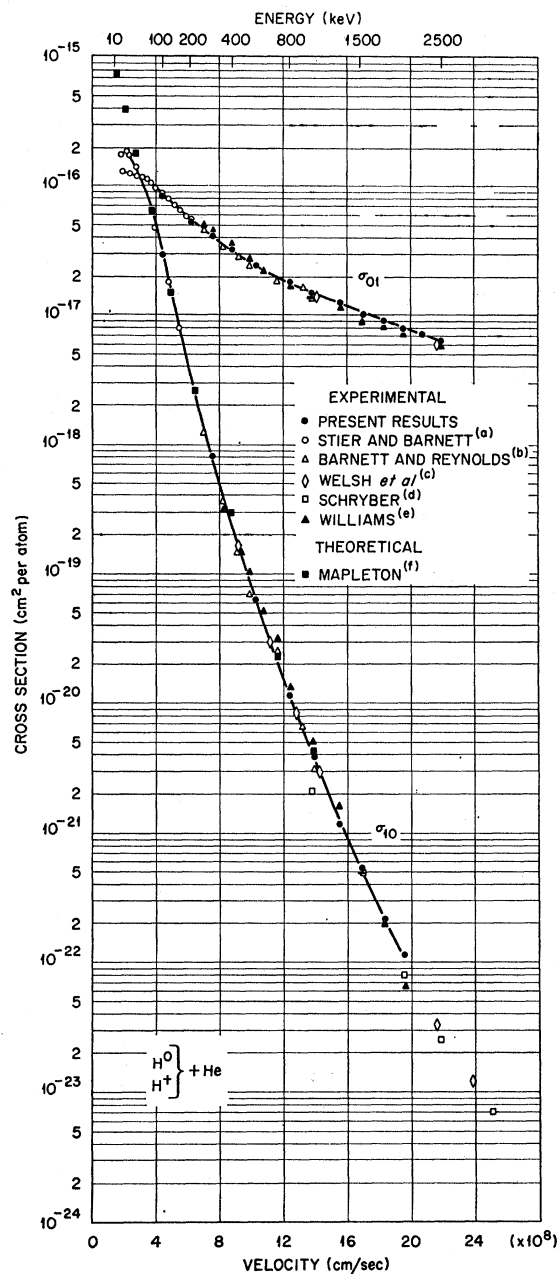


FIG. 3. Single-electron capture and loss cross sections for protons and atomic hydrogen, respectively, on helium with previous experimental and theoretical values. Experimental results: (a) see Ref. 17, (b) see Ref. 18, (c) see Ref. 2, (d) see Ref. 4, and (e) see Ref. 3. Theoretical results: (f) see Ref. 25.

(800 to 2500 keV) protons were obtained by means of a Van de Graaff generator. These proton energies were determined by a magnetic-resonance probe in the  $90^\circ$  analyzing magnet at the base of the Van de Graaff generator. This probe had previously been calibrated to  $\pm 0.5\%$  against the  ${}^7\text{Li}(p,n)$  threshold.

The apparatus used in the cross-section measurements is shown schematically in Fig. 1. Basically, the apparatus consists of two differentially pumped collision cells, two sets of electrostatic deflection plates, and detectors for the determination of the intensities of the neutral- and charged-beam components.

Circular apertures designated by a, b, c, c', and d in Fig. 1 were machined with thin edges to diameters of 0.010, 0.062, 0.020, 0.020, and 0.062 in., respectively. The dimensions of these apertures were selected in order to minimize scattering of the beam from the exit apertures of the collision cells. Pumping speed coupled with the dimensions of the apertures was such that a pressure differential of approximately 1500 was obtained across the apertures. Alignment of the system was made possible by means of bellows sections between the apertures.

The length of the first collision cell, defined by aper-

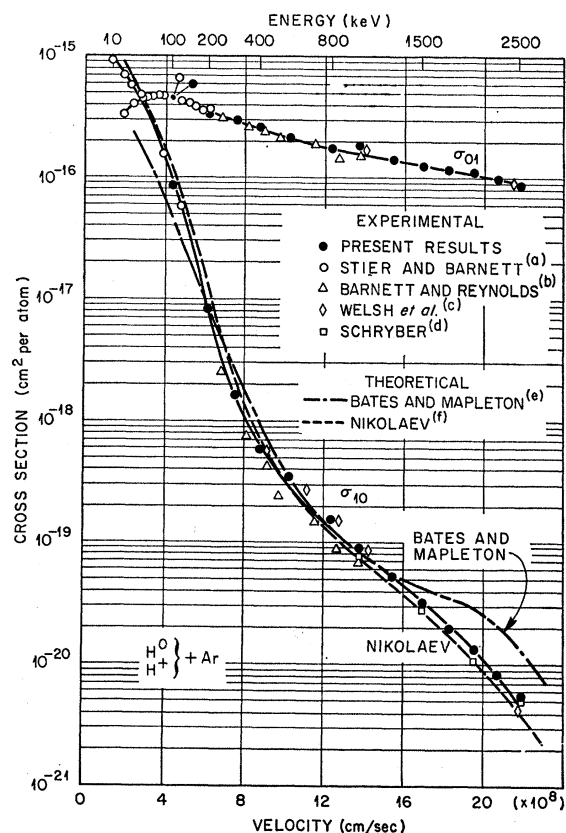


FIG. 4. Single-electron capture and loss cross sections for protons and atomic hydrogen, respectively, on argon with previous experimental and theoretical values. Experimental results: (a) see Ref. 17, (b) see Ref. 18, (c) see Ref. 2, and (d) see Ref. 4. Theoretical results: (e) see Ref. 14, and (f) see Ref. 12.

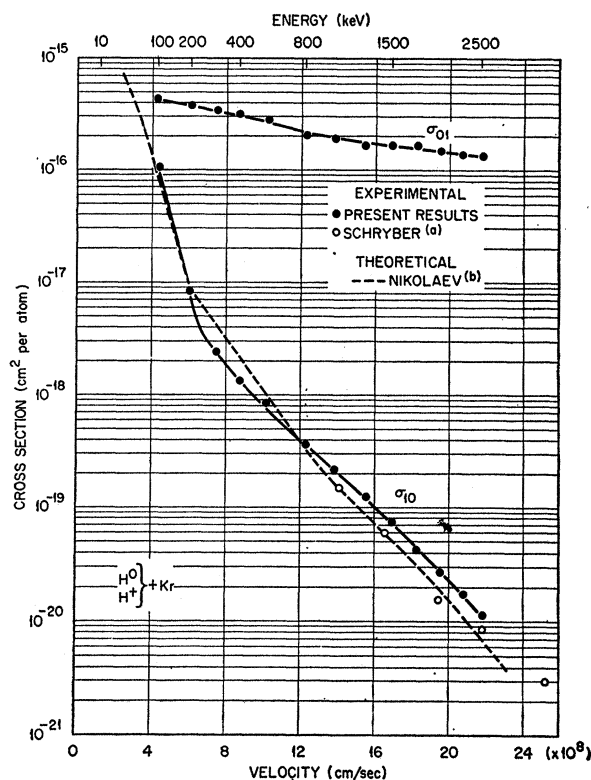


FIG. 5. Single-electron capture and loss cross sections for protons and atomic hydrogen, respectively, on krypton with previous experimental and theoretical results. Experimental results: (a) see Ref. 4. Theoretical results: (b) see Ref. 12.

tures a and b, was  $17.50 \pm 0.06$  in. Either argon or nitrogen gas was introduced into this cell for the production of a neutral beam which was formed by charge transfer of the incident proton beam with the gas in the cell. Following the first collision cell, the charged components of the beam were removed by applying an electric field to the deflection plates which left a beam of atomic hydrogen particles incident on the second collision cell. When a proton beam was desired, the first collision cell was evacuated and the first set of deflection plates was electrically grounded. The second collision cell, the target cell, was defined by apertures c and d to be  $17.50 \pm 0.06$  in. long. A modification made to the length of this cell during the experiment is shown by the dashed lines in Fig. 1. The length of the modified collision cell, defined by apertures c' and d, was  $3.06 \pm 0.06$  in.

The entire vacuum system (excluding the detector assembly) was made from stainless steel and assembled with metal O rings which enabled bake-out of the system at approximately  $200^\circ\text{C}$  by means of heater tapes wound around the vacuum chamber and insulated with asbestos.

Silicon-gold barrier detectors were used to measure both the neutral-beam component and the proton beam. These detectors had a sensitive area of approximately  $50 \text{ mm}^2$  and a depletion depth of approximately  $330 \mu$

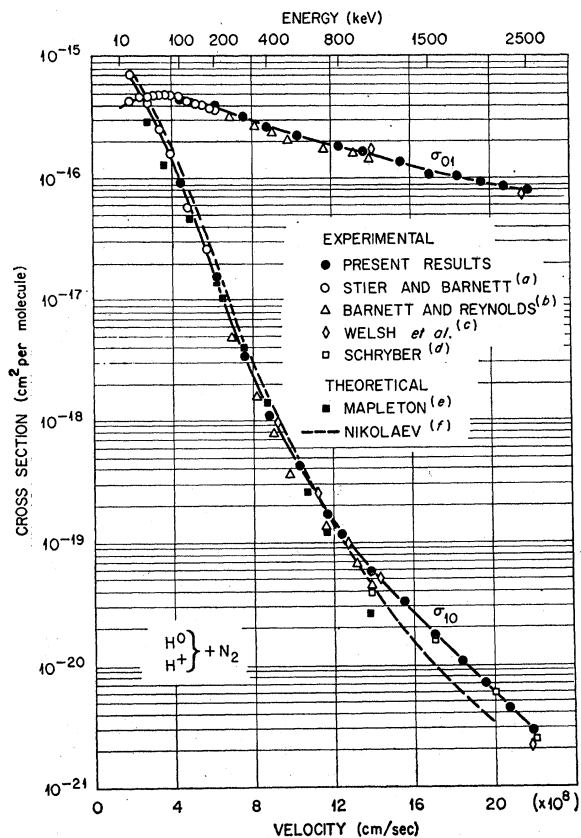


FIG. 6. Single-electron capture and loss cross sections for protons and atomic hydrogen, respectively, on nitrogen with previous experimental and theoretical results. Experimental results: (a) see Ref. 17, (b) see Ref. 18, (c) see Ref. 2, and (d) see Ref. 4. Theoretical results: (e) see reference 9 and (f) see reference 12.

(sufficient to stop 20-MeV protons). A Faraday cup was used to measure the proton current during that part of the experiment where high-intensity (greater than  $10^{-13}$  A) proton beams were needed.

The target-gas pressure was measured by means of a capacitance manometer. This device provided continuous pressure monitoring and pressure determinations which were independent of the nature of the gas. The pressure head was bakeable and had built-in thermostatically regulated heating elements for operation at constant temperature. The calibration was checked against a refrigerated McLeod gauge and found to agree to within  $\pm 3\%$  in the pressure range used for the cross-section measurements ( $1 \times 10^{-4}$  to  $1 \times 10^{-3}$  Torr). Full account was taken of systematic errors associated with the McLeod gauge.

#### IV. ERRORS

The uncertainties in the measured cross sections result primarily from the following factors: (1) the effective path length of the collision cell, (2) approximate corrections for deviations from "thin" target condi-

tions, (3) the measurement of target-gas pressures, (4) the measurement of beam intensities, (5) impurities in the target gases, and (6) possible excited states in the incident atomic hydrogen beam.

The effective path length is longer than the physical path length due to gas streaming from the apertures as a result of differential pumping. This effective increase in path length was estimated to be approximately 3% for the short cell and less than 1% for the long cell. These increases were arrived at from a comparison of the cross sections measured with each cell and by a simple calculation based on isotropic-molecular flow of gas from the apertures. The uncertainty associated with the length is estimated to be less than  $\pm 2\%$ .

An error resulted when cross sections were calculated using Eq. (3) because multiple collisions occurred between a single beam particle and the target gas. This error was corrected for and introduced a systematic uncertainty of less than  $\pm 2\%$ .

Uncertainties in the calibration in the capacitance manometer resulted in a possible systematic error of  $\pm 3\%$  in the measured target-gas pressure. The McLeod gauge with which this capacitance manometer was checked was cooled to  $0^\circ\text{C}$  to reduce the mercury stream-

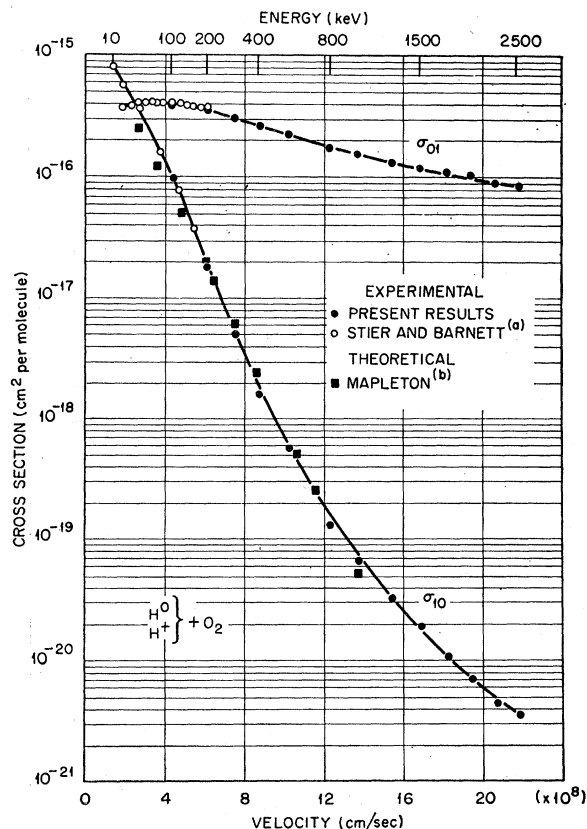


FIG. 7. Single-electron capture and loss cross sections for protons and atomic hydrogen, respectively, on oxygen with previous experimental and theoretical results. Experimental results: (a) see Ref. 17. Theoretical results: (b) see Ref. 9.

ing error and was thoroughly cleaned and outgassed. Only nitrogen and hydrogen gases were used in checking the calibration of the capacitance manometer. Uncertainties in the measurement of relative pressures due to meter fluctuations and small drifts in the pressure during data accumulation are estimated to be  $\pm 3\%$ .

The neutral-beam intensity and small ( $< 10^{-16}$  A) proton-beam intensities were measured by single-particle counting techniques. Sufficient data were accumulated to reduce counting statistics to less than 1%. Intense proton beams ( $> 10^{-13}$  A) were collected by a Faraday cup and measured by a Keithley model 410 micro-microammeter. The meter output was traced by a chart recorder to facilitate averaging this current. The random uncertainties in this averaging process were estimated to be less than 10% and the absolute calibration of the electrometer was measured accurate to  $\pm 2\%$ .

Random uncertainties in the cross sections due to the determination of beam intensities and target gas pressures can be evaluated best by the uncertainties encountered in obtaining the slope of a straight line through the points of a plot of intensity ratios versus pressure. This plot has a tendency to average the fluctuations for individual points when the cross section is

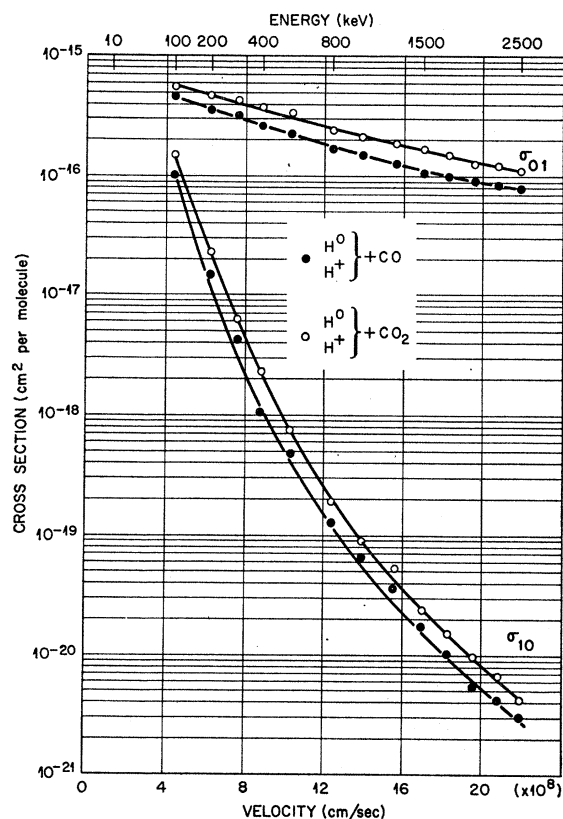


FIG. 8. Single-electron capture and loss cross sections for protons and atomic hydrogen, respectively, on carbon monoxide and carbon dioxide.

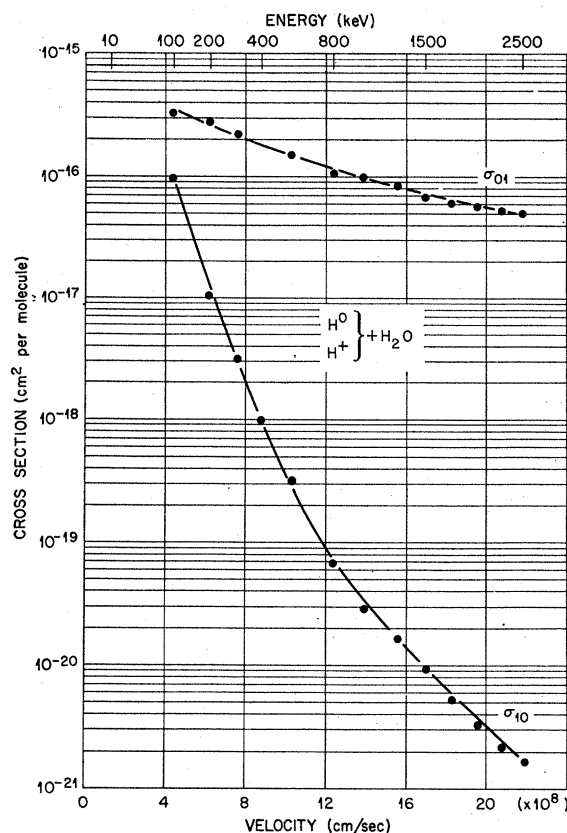


FIG. 9. Single-electron capture and loss cross sections for protons and atomic hydrogen, respectively, on water vapor.

calculated from the slope. The slope of each set of points corresponding to a particular cross section was determined by a least-squares fit. The uncertainties in the slopes of the straight lines vary from 3 to 5%. The larger uncertainty is associated with intensity data obtained by means of the Faraday cup.

The target gases, except water vapor, were purchased from commercial sources. The purity of these gases was better than 99.5% except  $\text{CO}_2$  which was 98.5% pure. The water vapor was from triply distilled water which had been evacuated by means of a forepump for 8 h while being frozen and thawed in order to remove absorbed gases. Hydrogen and helium were passed over a liquid-nitrogen cold trap before they were introduced into the target cell. The gases Ar,  $\text{N}_2$ ,  $\text{O}_2$ , CO,  $\text{CH}_4$ ,  $\text{C}_2\text{H}_4$ , and  $\text{C}_2\text{H}_6$  were passed through a cold trap at dry-ice temperature. The gases  $\text{CO}_2$ ,  $\text{H}_2\text{O}$ ,  $\text{C}_4\text{H}_{10}$ , and Kr were not trapped.

Since the neutral hydrogen beam is formed by electron capture, the existence of excited states in the beam must be considered. The majority of the excited states decay in the 65 cm distance between the first and second collision cells. The metastable  $2s$  state has a lifetime of a few milliseconds; however, this state was quenched by the perpendicular electric field used to deflect all charged

particles from the neutral beam.<sup>15</sup> The more highly excited states may have lifetimes long enough to reach the second collision chamber; however, since the population of excited states by electron capture is proportional to  $n^{-3}$ , the fraction of neutral particles in these highly excited states is negligible.

The combined effects of the uncertainties discussed above result in uncertainties in the measured electron-capture and electron-loss cross sections of 10 and 12%, respectively. The larger uncertainty results from the use of the Faraday cup.

## V. RESULTS AND DISCUSSION

Figures 2 through 11 show the present measured cross sections along with results from previous measurements and theoretical predictions.<sup>16</sup> The solid line on all the figures represents the line of best fit for the present results and, where applicable, includes the results of Stier and Barnett<sup>17</sup> at lower energies. Theoretical results for atomic targets were multiplied by 2 in order to compare them with the measured results for molecules.

Preliminary equilibrium fractions were measured during the initial phase of this experiment as a check of the internal consistency of the cross-section measurements. These equilibrium fractions were found to agree with the equilibrium fractions calculated from the measured cross sections to within 35%.

In Fig. 2 the previous measured results of Stier and Barnett,<sup>17</sup> Barnett and Reynolds,<sup>18</sup> Welsh *et al.*,<sup>2</sup> Schryber,<sup>4</sup> and Williams<sup>3</sup> are shown along with the present results. There is agreement between all the experimental values except for the results of Williams which are lower than the present results by 38% at 440 keV and by 75% at 175 keV. The values plotted in Ref. 3 contain a drafting error and are therefore multiplied by 2 and plotted in Fig. 2.<sup>19</sup>

Although many theoretical calculations exist for the charge-transfer process of protons on hydrogen atoms, only the calculation of Mapleton<sup>20</sup> is included in Fig. 2 in order to preserve clarity. In this calculation Mapleton used the Born approximation which included the probability of electron capture into seven final states of the projectile. This calculation agrees with present results. Other theoretical results of interest and their relation to the measured results are (1) the distorted-wave approximation of Basel and Gerjuoy<sup>21</sup> for capture into the ground state which tends to decrease slower than the present results at energies greater than 200 keV, (2) the

impact-parameter calculations of McCarroll<sup>22</sup> for ground-state capture which also tend to decrease slower than the present results, and (3) the Born-approximation calculation of Tuan and Gerjuoy<sup>23</sup> which includes the molecular effects of the H<sub>2</sub> target and tends to decrease faster than the present results.

The electron-loss cross section for atomic hydrogen on atomic hydrogen has been calculated by Bates and Griffing<sup>24</sup> using the first Born approximation. The calculated results and the present results agree at 100 keV but diverge at higher energies. At 2.5 MeV the calculated value is 150% larger than the present results.

The comparison of measured and calculated cross sections for a helium target, shown in Fig. 3, is similar to that described for hydrogen. At energies between 40 and 400 keV close agreement is obtained between experimental and theoretical values; however, for the electron-capture cross sections at higher energies discrepancies exist not only between theory and experiment, but also between theoretical results. Mapleton's results<sup>25</sup> of the first Born approximation, shown in Fig.

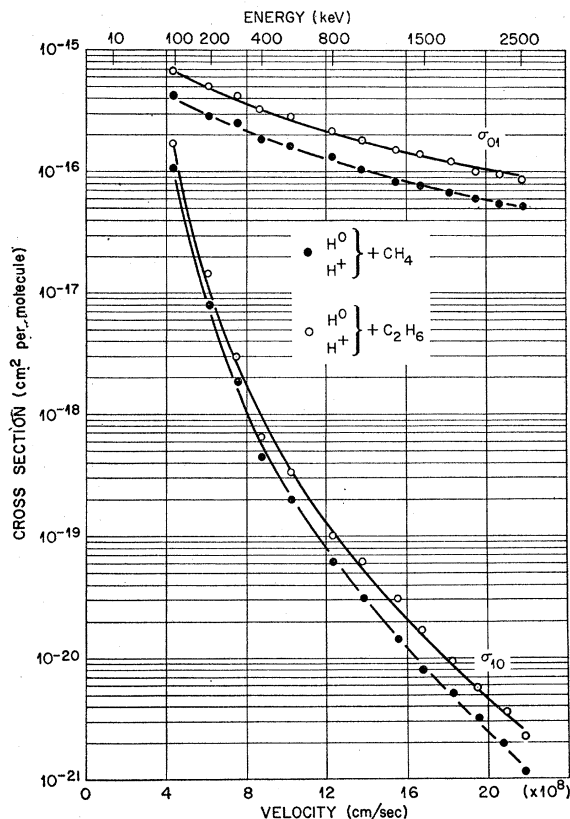


FIG. 10. Single-electron capture and loss cross sections for protons and atomic hydrogen, respectively, on methane and ethane.

<sup>15</sup> Wade L. Fite, in *Atomic and Molecular Processes*, edited by D. R. Bates (Academic Press Inc., New York, 1962), p. 421.

<sup>16</sup> Tabular results may be obtained from R.A.L. upon request.

<sup>17</sup> P. M. Stier and C. F. Barnett, *Phys. Rev.* **103**, 896 (1956).

<sup>18</sup> C. F. Barnett and H. K. Reynolds, *Phys. Rev.* **109**, 355 (1958).

<sup>19</sup> The abscissa of Fig. 3 of Ref. 3 should be labeled cross section, cm<sup>2</sup>/molecule; J. F. Williams (private communication).

<sup>20</sup> R. A. Mapleton, *Phys. Rev.* **126**, 1477 (1962).

<sup>21</sup> R. H. Bassel and E. Gerjuoy, *Phys. Rev.* **117**, 749 (1960).

<sup>22</sup> R. McCarroll, *Proc. Roy. Soc. (London)* **264**, 547 (1961).

<sup>23</sup> T. F. Tuan and E. Gerjuoy, *Phys. Rev.* **117**, 756 (1960).

<sup>24</sup> D. R. Bates and G. W. Griffing, *Proc. Phys. Soc. (London)* **A68**, 90 (1955).

<sup>25</sup> R. A. Mapleton, *Phys. Rev.* **122**, 528 (1961).

3, are in close agreement with the measured electron-capture cross sections above 40 keV, while the impulse-approximation calculations of Bransden and Cheshire<sup>26</sup> and the impact-parameter formulation of Bransden and Sin Fai Lam<sup>27</sup> bracket both the first Born calculation and the experimental points and differ from each other by approximately a factor of 2. The electron-loss cross-section calculation by Bates and Williams<sup>8</sup> agrees with the present results for energies between 10 and 300 keV but diverges at higher energies so that at 2.5 MeV the calculated cross section is 155% larger than the present measured result.

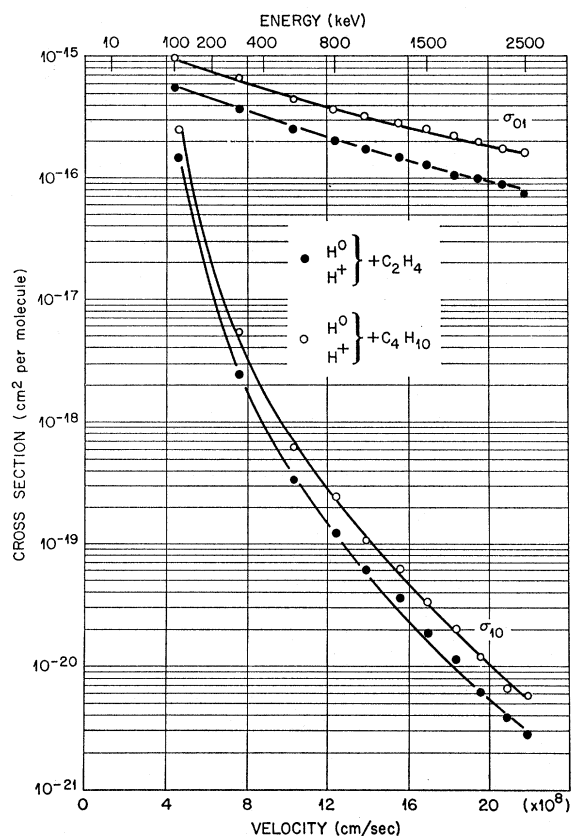


FIG. 11. Single-electron capture and loss cross sections for protons and atomic hydrogen, respectively, on ethylene and butane.

Results for the target gas argon are presented in Fig. 4. The present results of the electron-capture cross section are in agreement with the measurements of Stier and Barnett and Welsh *et al.*; however, the results of Barnett and Reynolds, and Schryber are up to 40% lower than the present results.

The apparent break at 800 keV in the curvature of the electron-capture cross section has been shown by Bates and Mapleton<sup>14</sup> and Nikolaev<sup>12</sup> to be caused by

<sup>26</sup> B. H. Bransden and I. M. Cheshire, Proc. Phys. Soc. (London), **81**, 820 (1963).

<sup>27</sup> B. H. Bransden and L. T. Sin Fai Lam, Proc. Phys. Soc. (London) **87**, 653 (1966).

TABLE I. Velocity dependence of the single-electron capture and loss cross sections.

Target gas	$k^a$			
	$200 \leq E < 400$ keV	$400 < E < 1000$ keV	$1000 < E \leq 2500$ keV	$300 < E \leq 2500$ keV
H <sub>2</sub>	10.6	10.6	10.6	1.70
He	9.7	9.7	9.7	1.76
Ar	7.1	4.4	7.1	0.98
Kr	7.0	<sup>b</sup>	7.0	0.98
N <sub>2</sub>	7.2	<sup>b</sup>	7.2	1.52
O <sub>2</sub>	6.9	6.9	6.9	1.20
H <sub>2</sub> O	7.2	7.2	7.2	1.40
CO	6.6	6.6	6.6	1.38
CO <sub>2</sub>	6.8	6.8	6.8	1.36
CH <sub>4</sub>	8.0	6.1	8.0	1.64
C <sub>2</sub> H <sub>4</sub>	8.0	5.7	8.0	1.52
C <sub>2</sub> H <sub>6</sub>	8.0	5.7	5.7	1.52
C <sub>4</sub> H <sub>10</sub>	6.8	5.6	6.8	1.46

<sup>a</sup>  $\sigma \propto v^{-k}$ .

<sup>b</sup> The value of  $k$  is continually changing in this energy region.

the effect of electron capture from inner electron shells of argon. The results of Bates and Mapleton shown in Fig. 4 are from a semiclassical calculation which includes the effects of inner-shell electron capture. Their calculated values appear to overestimate the high-energy capture cross sections. Nikolaev has included inner-shell-capture contributions in his first Born calculation and his results are in close agreement with the measured values.

The cross sections for krypton are shown in Fig. 5. The break in the curvature of the electron-capture cross sections at 200 keV due to inner-shell capture is also reflected in the calculated results of Nikolaev. At energies greater than approximately 1.0 MeV the results of Nikolaev, as well as the measurements of Schryber, are nearly 40% lower than the present results.

Results for the target-gas nitrogen are shown in Fig. 6. The results of Stier and Barnett agree well with the present results through the energy overlap region. The present results agree with the results of Welsh *et al.* for energies less than 1 MeV. For all energies greater than 500 keV the present results for the electron-capture cross section are from 10 to 50% higher than the corresponding measurements of Barnett and Reynolds and of Schryber. The calculated electron-capture cross sections of Nikolaev which include the probability of inner-shell capture are in close agreement with our measured values at low energies; however, for energies greater than 500 keV, his results are lower by 20 to 50%. The calculated values of Mapleton<sup>9</sup> are in close agreement with experiment for energies from 100 to 300 keV. His results fall off more rapidly than the measured values for higher energies since this calculation is only for  $2p$  electron capture. A later calculation by Mapleton<sup>11</sup> includes inner-shell contributions and these results overestimate the cross sections.

The data for oxygen are shown in Fig. 7. The only previous experimental results are those of Stier and Barnett for low energies. In the energy region of overlap

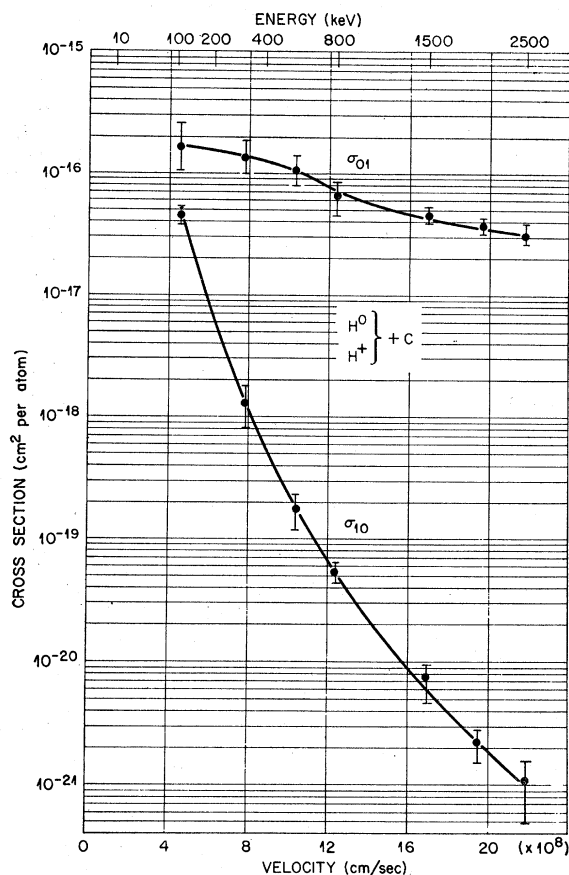


FIG. 12. Single-electron capture and loss cross sections for protons and atomic hydrogen, respectively, on carbon as calculated by the sum rule.

the agreement between these measured values is quite good. The calculated capture cross sections of Mapleton<sup>9</sup> agree with the present measurements up to energies near 800 keV. At higher energies agreement is not expected as inner-shell capture contributions are not included in his calculation.

Fig. 8 through 11 show the measured cross sections for the gases CO, CO<sub>2</sub>, H<sub>2</sub>O, CH<sub>4</sub>, C<sub>2</sub>H<sub>4</sub>, C<sub>2</sub>H<sub>6</sub>, and C<sub>2</sub>H<sub>10</sub>. The similar shape of the cross sections for each of the gases is reflected in the velocity dependence de-

termined by the line of best fit for each gas and listed in Table I. For energies greater than approximately 300 keV the electron-loss cross sections fit a power law very well. The electron-capture cross sections show departures from a strict power law near the energies predicted for the onset of capture from inner shells. This departure from a strict power law is indicated by the variation of the velocity dependence with energy as shown in Table I.

Using the measured cross sections of the various carbon-containing compounds it is possible to estimate the charge-transfer cross sections for carbon by applying an additive rule to the cross sections of each compound. The possibility of using this procedure is based on the assumption that, at high velocities of the incident particle, the target molecule appears as an assembly of individual atoms such that molecular forces are negligible. The carbon cross sections were calculated by the sum rule from the cross sections measured for the gases H<sub>2</sub>, O<sub>2</sub>, CO<sub>2</sub>, CH<sub>4</sub>, C<sub>2</sub>H<sub>4</sub>, C<sub>2</sub>H<sub>6</sub>, and C<sub>4</sub>H<sub>10</sub>. The results of this calculation are shown in Fig. 12 where the uncertainties in each point reflect the range of carbon cross sections obtained from different carbon-containing compounds. It must be emphasized that, although the sum rule gives surprisingly consistent results, it is only an estimate and the effects of molecular forces on the measured cross sections are observed for incident-particle energies as high as 2.5 MeV.

#### ACKNOWLEDGMENTS

We wish to thank J. G. Carter and E. T. Loy for their work on the initial design and construction of the charge-transfer apparatus. We also wish to thank A. Kenerly, J. A. Harter, and J. A. Ray for their assistance in the assembly and operation of the electronic equipment. Thanks are also extended to J. P. Judish and W. C. H. White for their assistance in the operation of the Van de Graaff accelerator. The authors are deeply indebted to C. F. Barnett and R. D. Birkhoff for many valuable discussions throughout this research and in the preparation of this paper. One of us (L.H.T.) received financial support from an Oak Ridge Graduate Fellowship administered by the Oak Ridge Associated Universities.